Journal of Economic Behavior & Organization 75 (2010) 77–94

Contents lists available at ScienceDirect

Journal of Economic Behavior & Organization

journal homepage: www.elsevier.com/locate/jebo

Regular and chaotic growth in a Hicksian floor/ceiling model

Iryna Sushko[a], Laura Gardini[b,*], Tönu Puu[c]

[a] Institute of Mathematics, National Academy of Sciences of Ukraine, and Kyiv School of Economics, Kiev, Ukraine
[b] Department of Economics and Quantitative Methods, University of Urbino, Italy
[c] Centre for Regional Science, Umeå University, Sweden

ARTICLE INFO

Article history:
Received 23 July 2008
Received in revised form 18 January 2010
Accepted 26 January 2010
Available online 6 February 2010

PACS:
02.30.Oz
05.45.-a

Keyword:
Hicksian model

ABSTRACT

In some previous papers the present authors reassembled the Hicksian trade cycle model in a new way. The floor was tied to depreciation on capital, itself the cumulative sum of past net investments, for which the principle of acceleration provided an explanation. Hence no alien elements were needed to include capital, and so close the system. The resulting model created a growth trend along with growth rate cycles, which could be periodic or quasiperiodic. In the current paper, the ceiling, using capital stock as a capacity limit for production, is added. It then turns out that pure growth no longer exists, and chaos and multistability become possible, which they were not in the previous model. A variety of bifurcation scenarios is explored, and a full understanding of the working of the four-piece, originally three-dimensional, piecewise smooth map, is attained, using a reduction to a one-dimensional return map.

1. Introduction

1.1. Background

In this paper the Hicksian floor–ceiling model of the business cycle is reconsidered. As we know, the multiplier-accelerator model invented by Samuelson (1939) and also used by Hicks (1950) could produce either pure growth or cycles, depending on the parameters. In Samuelson's linear format the model (whether the solution was cyclic or growing/declining) would either explode or else extinguish any initially present motion. The Hicksian floor and ceiling, which made the model non-linear, introduced the possibility of sustained cyclic variation.

However, there could still be *either* growth or cycles, never both. Therefore Hicks added an *exogenous* growth trend in terms of autonomous expenditures, around which the multiplier-accelerator model produced sustained cycles bounded by the floor (lower bound to disinvestment) and ceiling (upper capacity bound to production).

In Puu et al. (2005) the possibility of making growth endogenous was explored. As the floor is a limit to disinvestment, representing the decrease in the capital stock occurring when no worn out capital at all was replaced, it was suggested to link it to the actual capital stock through an assumed rate of depreciation. Capital was not a variable in Hicks's original model, but, as capital is nothing but the cumulative sum of its increments, i.e., investments, for which there was a theory in the model, no alien elements were needed for inclusion of the capital variable, thus closing the model. The advantage was that the model now created an *endogenous growth* trend along with *cycles in the growth rates*. At the same time the growth rates in the cyclic regimes, which had been enormous in the original model, were reduced to but a fraction, which adds one feature of realism to the, still admittedly, much oversimplified model.

* Corresponding author. Tel.: +39 0722 305510; fax: +39 0722 305550.
E-mail address: gardini@econ.uniurb.it (L. Gardini).

0167-2681/$ – see front matter © 2010 Elsevier B.V. All rights reserved.
doi:10.1016/j.jebo.2010.01.007

Growing models are not readily analyzed by standard methods, so the model in Puu et al. (2005) was converted to new "relative" variables, the growth factor and the capital to income ratio. This, however, made the original piecewise linear model non-linear, but also had the advantage of reducing its dimension from three to two.

The model with floor only, retained the unrealistic feature that with high accelerators it still created pure exponential growth. Therefore, in Puu (2007) a ceiling along Hicks's original line of thought was added. The simplest argument behind the principle of acceleration is a fixed coefficient limitational production technology that makes producers use capital and other inputs in strict proportion to the output. The same idea could, however, also be used for an upper limit (ceiling) to possible output (=real income), again making use of the capital variable. In Puu (2007) it was proved that no more pure growth points did exist as possible trajectories of the model. However, although producing some exemplifying trajectories and bifurcation diagrams, which hinted at the possibility of complex results (such as chaos), the model remained mathematically largely unexplored. To carry out such a mathematical analysis is the objective of the present paper.

1.1.1. The Samuelson model

"Multiplier theory" assumes consumption to be a given fraction, c, of income, i.e., $C_t = cY_{t-1}$, where a one period lag is allowed for consumption out of incomes earned the preceding period.[1]

The "principle of acceleration" determines investment. The idea is that capital is needed in a fixed proportion, a, to the (real) income to be produced, i.e., $K_t = aY_{t-1}$, where again a one period lag is allowed for the building up of capital. As investments are the change of capital stock, i.e., $I_t = K_t - K_{t-1}$, we have $I_t = a(Y_{t-1} - Y_{t-2})$.[2]

Plugging $I_t = a(Y_{t-1} - Y_{t-2})$ and $C_t = cY_{t-1}$ into

$$Y_t = C_t + I_t, \tag{1}$$

the reduced form equation:

$$Y_t = (c + a)Y_{t-1} - aY_{t-2} \tag{2}$$

is obtained, which is Hicks's version of the original Samuelson model.[3]

1.1.2. Hicksian floor and ceiling

The floor: According to $I_t = a(Y_{t-1} - Y_{t-2})$ investments become negative when income is decreasing. However, disinvestment cannot exceed the natural depreciation on capital in the absence of any reinvestment to replace worn out capital. For this reason Hicks introduced a lower bound for disinvestment $-I_t^f$. Accordingly, the principle of acceleration took the form

$$I_t = \max(a(Y_{t-1} - Y_{t-2}), -I_t^f) \tag{3}$$

The Ceiling: The ceiling is motivated as follows. Given income is growing very fast, some resources may become limiting, so there is also a ceiling for income Y_t^c, and the income formation Eq. (1) is replaced by:

$$Y_t = \min(C_t + I_t, Y_t^c) \tag{4}$$

Using the consumption function $C_t = cY_{t-1}$ in (4) and substituting from (3), we obtain the new reduced form:

$$Y_t = \min(cY_{t-1} + \max(a(Y_{t-1} - Y_{t-2}), -I_t^f), Y_t^c) \tag{5}$$

which replaces (2).

1.1.3. Capital formation

Before leaving the original model let us check that it contained a capital formation theory, though it was never stated explicitly, as it did not feed back into the original model. From the definition of investments $I_t = K_t - K_{t-1}$, we have

$$K_t = K_{t-1} + I_t$$

so, using (3),

$$K_t = K_{t-1} + \max(a(Y_{t-1} - Y_{t-2}), -I_t^f) \tag{6}$$

which is an updating equation for capital.

---

[1] The accounting identity reads $Y_t = C_t + I_t$, or $Y_t = cY_{t-1} + I_t$. In equilibrium, $Y_t = Y_{t-1}$, so $Y_t = (1/1 - c)I_t$. As $c < 1$, the factor $(1/1 - c) > 1$ multiplies up investment expenditures, whence the term multiplier.

[2] Assume an aggregate production function $\bar{Y}_t = \min(\bar{K}_{t-1}/a, \bar{L}_{t-1}/b)$, where $\bar{K}_{t-1}$ and $\bar{L}_{t-1}$ denote *planned* capital and labour, needed for producing output $\bar{Y}_t$, *expected* to be demanded at the end of period t. Further, assume a naive forecasting rule $\bar{Y}_t = Y_{t-1}$, that the formation of capital takes exactly one period, i.e. $K_t = \bar{K}_{t-1}$, and that labour supply is affluent and it hence is the availability of capital that is binding. We have $K_t = aY_{t-1}$.
According to definition, investment becomes $I_t = K_t - K_{t-1} = a(Y_{t-1} - Y_{t-2})$, which justifies the principle of acceleration.

[3] To be quite true to history, Samuelson (1939) applied the accelerator to consumption only, i.e., assumed $I_t = a(C_{t-1} - C_{t-2})$. It was Hicks (1950) that replaced consumption by income.

1.2. A suggested reformulation

1.2.1. The floor

In Puu et al. (2005) it was suggested to relate the floor to the stock of capital through a depreciation factor r. Then, $I_t^f = rK_{t-1}$, so the investment function becomes

$$I_t = \max(a(Y_{t-1} - Y_{t-2}), -rK_{t-1}). \tag{7}$$

Using (7) in the income formation Eq. (1) along with $C_t = cY_{t-1}$, we get

$$Y_t = cY_{t-1} + \max(a(Y_{t-1} - Y_{t-2}), -rK_{t-1}). \tag{8}$$

Further, using $I_t^f = rK_{t-1}$ in (6),

$$K_t = K_{t-1} + \max(a(Y_{t-1} - Y_{t-2}), -rK_{t-1}). \tag{9}$$

Eqs. (8) and (9) provide a complete dynamical system in the two variables Y_t, K_t. It is actually third order as the right hand sides contain also income, delayed two periods.

1.2.2. The ceiling

The ceiling was skipped in Puu et al. (2005), but reintroduced in Puu (2007), putting $Y_t^c = K_{t-1}/a$. Accordingly, with proper substitution also for $I_t^f = rK_{t-1}$ (5) becomes[4]:

$$Y_t = \min(cY_{t-1} + \max(a(Y_{t-1} - Y_{t-2}), -rK_{t-1}), \frac{1}{a}K_{t-1}), \tag{10}$$

replacing (8), whereas (9) remains as it is.

The new map contains two maximum/minimum clauses, and hence consists of four pieces, each of which is a linear map.

1.2.3. The resulting map

In order to decide which selection in the min/max choice applies we need three conditions. The condition for application of the floor can be stated in terms of the quantity

$$R_{t-1} = a(Y_{t-1} - Y_{t-2}) + rK_{t-1} \tag{11}$$

When $R_{t-1} \geq 0$ then the multiplier-accelerator process works, whereas if $R_{t-1} < 0$, then the floor is activated.

As for the applicability of the ceiling, we check whether the sum of consumption cY_{t-1} and investments (accelerator generated as $a(Y_{t-1} - Y_{t-2})$, or fixed at floor level $-rK_{t-1}$), exceeds the maximum production capacity $(1/a)K_{t-1}$ or not, so let us define:

$$S_{t-1} = (c + a)Y_{t-1} - aY_{t-2} - \frac{1}{a}K_{t-1}, \tag{12}$$

and

$$T_{t-1} = cY_{t-1} - rK_{t-1} - \frac{1}{a}K_{t-1}. \tag{13}$$

If $R_{t-1} \geq 0$ and $S_{t-1} \leq 0$, then the classical multiplier-accelerator process works as usual, whereas for $R_{t-1} < 0$ and $T_{t-1} > 0$ we deal with the case where both floor and ceiling are applied at the same time. The conditions in terms of (11)–(13) are not independent, because $S_{t-1} - T_{t-1} \equiv R_{t-1}$, however this does not simplify the map, as the phase space is always split into eight parts,[5] and the map becomes

$$\begin{cases} K_t = K_{t-1} + a(Y_{t-1} - Y_{t-2}) \\ Y_t = \dfrac{1}{a}K_{t-1} \end{cases} \quad R_{t-1} \geq 0, S_{t-1} > 0, \tag{14}$$

$$\begin{cases} K_t = K_{t-1} + a(Y_{t-1} - Y_{t-2}) \\ Y_t = cY_{t-1} + a(Y_{t-1} - Y_{t-2}) \end{cases} \quad R_{t-1} \geq 0, S_{t-1} \leq 0, \tag{15}$$

$$\begin{cases} K_t = (1 - r)K_{t-1} \\ Y_t = cY_{t-1} - rK_{t-1} \end{cases} \quad R_{t-1} < 0, T_{t-1} \leq 0, \tag{16}$$

[4] We again use the production function $Y_t = \min(K_{t-1}/a, L_{t-1}/b)$. The dating is different from its use above, but now we deal with *actual* quantities, not with planned and expected. Supposing capital is again binding, we must have $Y_t \leq K_{t-1}/a$.

[5] Notice that three independent planes in a three-dimensional phase pace divide it into eight different regions.

$$\begin{cases} K_t = (1-r)K_{t-1} \\ Y_t = \dfrac{1}{a}K_{t-1} \end{cases} \qquad R_{t-1} < 0, T_{t-1} > 0, \tag{17}$$

The first map represents the case with the ceiling activated, the third the one with the floor activated, the second is the regular multiplier-accelerator model, whereas the last is case where both the floor and ceiling constraints are activated at once.

In the model we have three parameters with the ranges $0 < c < 1$, $0 < a$, and $0 < r < 1$.

1.3. The relative system

As in Puu et al. (2005), we now convert the system (14)–(17) to a relative system, in order to obtain stationary orbits, using

$$y_t = \frac{Y_t}{Y_{t-1}} \tag{18}$$

and

$$k_t = \frac{K_t}{Y_{t-1}} \tag{19}$$

for the income growth ratio and the capital to income ratio respectively.

Through the conversion all the branches become second order. In order to define the branch conditions (11)–(13) properly in terms of y_t, k_t, we multiply them through by the factor K_{t-1}/Y_{t-2}^2, which is granted to be nonnegative, and define $\rho_t = R_t K_t/Y_{t-1}^2$, $\sigma_t = S_t K_t/Y_{t-1}^2$ and $\varsigma_t = T_t K_t/Y_{t-1}^2$, so that we get:

$$\rho_{t-1} = a(y_{t-1} - 1)k_{t-1} + rk_{t-1}^2, \tag{20}$$

$$\sigma_{t-1} = (c + a)y_{t-1}k_{t-1} - ak_{t-1} - \frac{1}{a}k_{t-1}^2, \tag{21}$$

$$\varsigma_{t-1} := cy_{t-1}k_{t-1} - rk_{t-1}^2 - \frac{1}{a}k_{t-1}^2, \tag{22}$$

with the resulting maps

$$\begin{cases} k_t = \dfrac{k_{t-1}}{y_{t-1}} + a\left(1 - \dfrac{1}{y_{t-1}}\right) \\ y_t = \dfrac{1}{a}\dfrac{k_{t-1}}{y_{t-1}} \end{cases} \qquad \rho_{t-1} \geq 0, \sigma_{t-1} > 0, \tag{23}$$

$$\begin{cases} k_t = \dfrac{k_{t-1}}{y_{t-1}} + a\left(1 - \dfrac{1}{y_{t-1}}\right) \\ y_t = c + a\left(1 - \dfrac{1}{y_{t-1}}\right) \end{cases} \qquad \rho_{t-1} \geq 0, \sigma_{t-1} \leq 0, \tag{24}$$

$$\begin{cases} k_t = (1-r)\dfrac{k_{t-1}}{y_{t-1}} \\ y_t = c - r\dfrac{k_{t-1}}{y_{t-1}} \end{cases} \qquad \rho_{t-1} < 0, \varsigma_{t-1} \leq 0, \tag{25}$$

and

$$\begin{cases} k_t = (1-r)\dfrac{k_{t-1}}{y_{t-1}} \\ y_t = \dfrac{1}{a}\dfrac{k_{t-1}}{y_{t-1}} \end{cases} \qquad \rho_{t-1} < 0, \varsigma_{t-1} > 0. \tag{26}$$

2. Description of the map

Summing up, we consider the two-dimensional nonlinear discontinuous piecewise smooth map F given by four maps F_i, $i = 1, 2, 3, 4$:

$$F : (k, y) \mapsto \begin{cases} F_1(k, y), & \rho \geq 0, \sigma > 0, \\ F_2(k, y), & \rho \geq 0, \sigma \leq 0, \\ F_3(k, y), & \rho < 0, \zeta \leq 0, \\ F_4(k, y), & \rho < 0, \zeta > 0, \end{cases} \tag{27}$$

where the maps F_i are defined as follows:

$$F_1 : \begin{pmatrix} k \\ y \end{pmatrix} \mapsto \begin{pmatrix} k/y + a(1 - 1/y) \\ k/ay \end{pmatrix},$$

$$F_2 : \begin{pmatrix} k \\ y \end{pmatrix} \mapsto \begin{pmatrix} k/y + a(1 - 1/y) \\ c + a(1 - 1/y) \end{pmatrix},$$

$$F_3 : \begin{pmatrix} k \\ y \end{pmatrix} \mapsto \begin{pmatrix} k(1 - r)/y \\ c - kr/y \end{pmatrix},$$

$$F_4 : \begin{pmatrix} k \\ y \end{pmatrix} \mapsto \begin{pmatrix} (1 - r)k/y \\ k/ay \end{pmatrix},$$

and ρ, σ, ζ are given in (20)–(22), respectively (omitting the lower index $t - 1$). The parameters a, c and r are real and such that $0 < c < 1$, $0 < r < 1$, and $a > 0$. Let us first remark that in this work we are only interested to the case $a > 1$. In fact, when the parameter a satisfies $0 < a < 1$ then the model in the original variables has the fixed point in the origin which is asymptotically stable and at $a = 1$ a bifurcation occurs (a center bifurcation, conjugate eigenvalues crossing the unit circle), after which the dynamics are diverging. Correspondingly, in the relative model for $0 < a < 1$ the trajectories are diverging and at $a = 1$ a particular bifurcation occurs (involving the points at infinity, on the Poincaré Equator). While we are interested in situations in which the fixed point in the origin of the original model is unstable and endogenous cycles appear of increasing amplitude, that is what occurs for $a > 1$, and in order to study the trend of the diverging trajectories we have introduced the relative model described above. In it, for $a > 1$ we can have bounded trajectories which allow us to study how the trajectories in the original model are growing. Thus it is this last regime of interest to us, and in this paper we restrict our analysis to the case $a > 1$.

Let R_i, $i = 1, 2, 3, 4$, denote the regions of definition of the maps F_i. The boundaries of R_i are defined by four straight lines, which we call critical lines and denote as $L_{-1}^{(i)}$:

$$L_{-1}^{(1)} = \left\{(k, y) : y = 1 - rk/a\right\};$$

$$L_{-1}^{(2)} = \left\{(k, y) : y = (a^2 + k)/a(c + a)\right\};$$

$$L_{-1}^{(3)} = \left\{(k, y) : y = (ra + 1)k/ac\right\};$$

$$L_{-1}^{(4)} = \left\{(k, y) : k = 0\right\}.$$

The function F is defined in the whole plane except for the axis $y = 0$. The image of a point on the axis $y = 0$ is at infinity, i.e. belongs to the so-called Poincaré Equator; thus the iterative dynamic process is well defined in the real phase plane, except for this axis and all its preimages[6] of any rank. The map F is continuous on $L_{-1}^{(1)}$, $L_{-1}^{(2)}$, $L_{-1}^{(3)}$ and discontinuous on $L_{-1}^{(4)}$. The qualitative picture of the partition of the (k, y)-phase plane into the regions R_i (for parameters in the range of interest) is shown in Fig. 1.

The dynamic behavior of the map defined only by the two functions F_2 (for $\rho \geq 0$) and F_3 (for $\rho < 0$) was studied in Sushko et al. (2004) and Sushko and Gardini (2009). In particular, in Sushko and Gardini (2009) it is shown that at $a = 1$ the fixed point of F_2 located on the Poincaré Equator undergoes the center bifurcation, giving rise to an attracting invariant one-dimensional set in the phase plane on which the map F can have, depending on parameters, either a pair of cycles of any period $n \geq 6$ (one attracting and one saddle), or a quasiperiodic trajectory. The dynamics of the map F given in (27) can be more complicated: even chaotic. To give a general view of the asymptotic behavior of F we show two bifurcation diagrams

[6] We recall that given a map $X_{n+1} = T(X_n)$ a preimage of rank-one of a point P is any point Q which satisfies $P = T(Q)$ (see Mira et al., 1996).

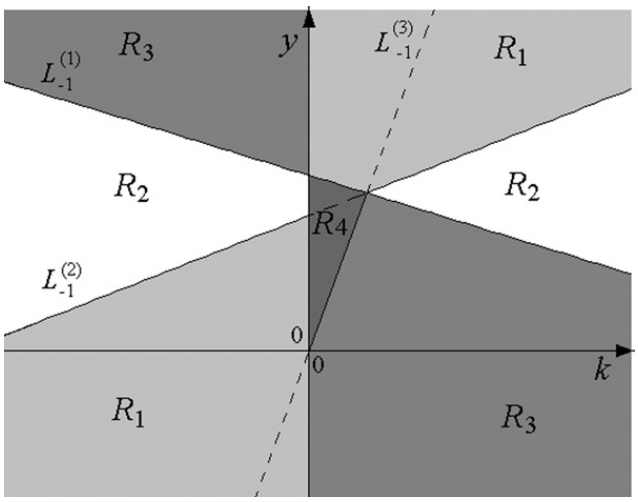

Fig. 1. Regions of definition in the phase plane.

for F in the (a, c)-parameter plane for $r = 0.025$ (Fig. 2) and $r = 0.3$ (Fig. 3). Regions related to attracting cycles of different periods $n \leq 42$ are shown by different shades of gray, and the white region corresponds to either cycles of period $n > 42$, or to chaotic trajectories. It is also shown a curve $c = c^*$ obtained numerically, corresponding to a contact of the attractor with the boundary $L_{-1}^{(2)}$ of the region R_1, where the map F_1 is defined. For $c < c^*$ only the two maps F_2 and F_3 are involved in the asymptotic dynamics of F (which is as already described in Sushko et al. (2004)). The purpose of the present paper is to study the dynamics of F for $c > c^*$ and to explain some different mechanisms of transition to chaos.

Appendix A contains a short description of the four map components of F, together with a description of the application of the map F to the regions R_i, $i = 1, \ldots, 4$. The result is summarized in Fig. 4, and the analytic expressions for the boundaries of the regions are given in Appendix A.

The white region in Fig. 4 denotes the locus of points which are never visited by a trajectory (the so-called region Z_0), while the points in the gray (respectively white hatched) regions have two (respectively one) preimages.

It is immediately seen that the region R_4 is never involved in the asymptotic dynamics (as any point from that region is mapped outside, and its orbit never reenters the same region). Neither does the discontinuity line $k = 0$ have any influence on the asymptotic dynamics of the map F. Thus we are left with the dynamics of the points belonging to the three remaining regions. We know that if the regions involved are only R_2 and R_3 (i.e. only the maps F_2 and F_3) then the dynamics are regular, whereas, as we shall see, the new region R_1 will play an important role in producing more spectacular phenomena.

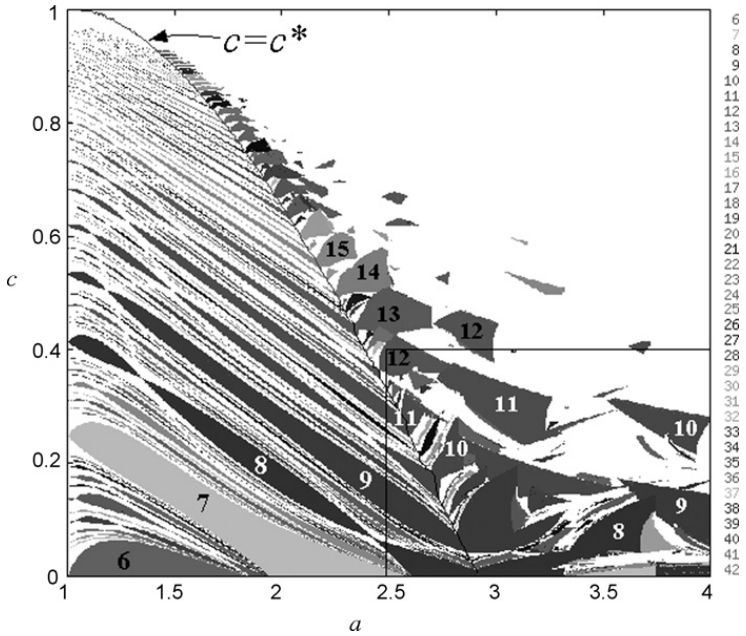

Fig. 2. Two-dimensional bifurcation diagram in the (a, c)-parameter plane at $r = 0.025$.

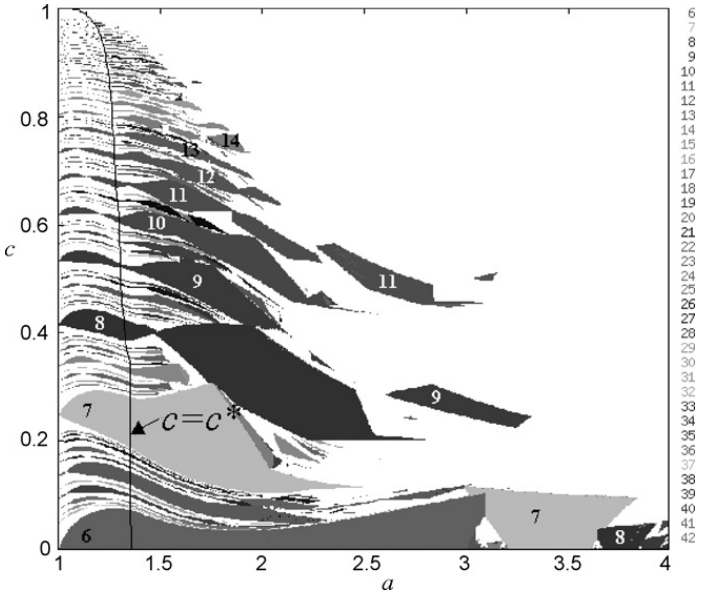

Fig. 3. Two-dimensional bifurcation diagram in the (a, c)-parameter plane at $r = 0.3$.

In order to understand which maps are involved in the asymptotic dynamics of F, and how, let us first assume that a trajectory has a point $(k_j, y_j) \in R_3$. Then $(k_{j+1}, y_{j+1}) = F_3(k_j, y_j) \in L_0^{(1)}$, as F_3 maps all the points into the line $L_0^{(1)}$.

For $c < 1 - r$ the attracting fixed point of F_3 is $(k^*, 1 - r) \in R_2$, where $k^* = (1 - r)(c - 1 + r)/r < 0$, and the repelling fixed point $(0, c)$ is just on the border of R_2 (see Appendix A). Thus, approaching the attracting fixed point, the trajectory necessarily enters the region R_2, i.e., there exists some $s > 0$ such that $(k_{j+1+s}, y_{j+1+s}) \in L_0^{(1)} \subset R_2$, where $k_{j+1+s} < 0$.

If $c > 1 - r$, then the fixed point $(0, c)$ is attracting, while $(k^*, 1 - r)$ with $k^* > 0$ is repelling, thus also in this case the above conclusion holds. So, we have $(k_{j+1+s}, y_{j+1+s}) \in R_2$.

The trajectory cannot stay forever in R_2, given that, as it is shown in Sushko and Gardini (2009) (see also Appendix A), for $c < c^{**} = 2\sqrt{a} - a$, $a > 1$, the map F_2 has a transversely attracting invariant straight line $\{x = a\}$, on which the trajectory of any point is either periodic, or quasiperiodic under the map F_2. It is shown that any such trajectory must have at least one point in R_3, thus, it cannot stay forever in R_2. For $c > c^{**}$ the fixed points of F_2, located at $\{x = a\}$, belong to R_1. Thus, the trajectory must enter other regions, that is either R_1 or R_3. Indeed, there are two possibilities:

- The trajectory never enters the region R_1 (which occurs in the parameter range $c < c^*$ in Figs. 2 and 3). This means that, after a number of consecutive points in R_2 with $k < 0$, $y > 0$ the trajectory enters the subregion of R_2 below $y = 0$ and above a straight line which is the preimage of $L_{-1}^{(2)}$ by F_2, i.e., above the straight line $L_{-2}^{(2)} = F_2^{-1}(L_{-1}^{(2)})$. Points of this subregion are mapped in the subregion of R_2 below $L_{-1}^{(2)}$ and above $y = c + a$. Then, after some number of iterations under F_2 the

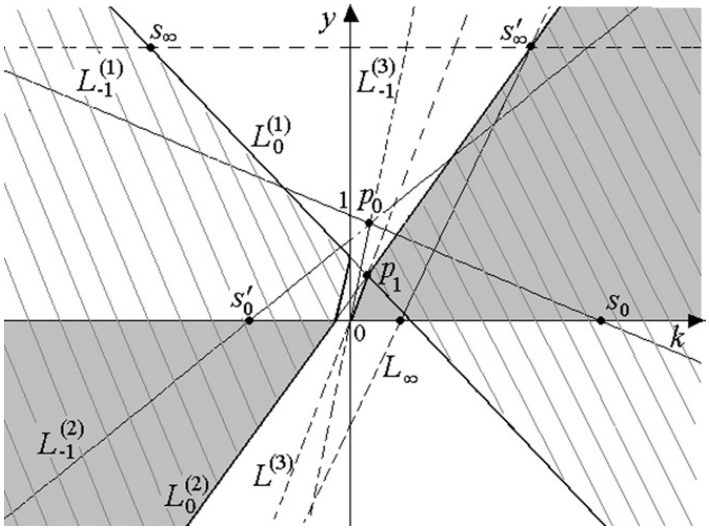

Fig. 4. Image of the phase plane in one application of the map F.

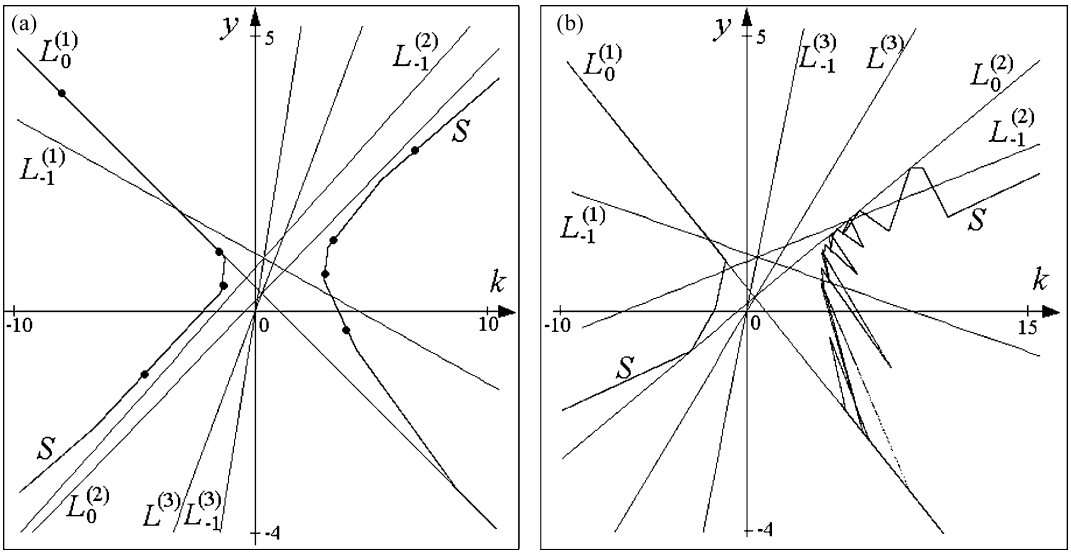

Fig. 5. Examples of the two-branch attracting invariant set S for $r = 0.3$, $c = 0.41$, $a = 1.25$ (a) and $a = 2.5$ (b). In (a) also shown are points of the attracting cycle of period 8 of the map F, while in case (b) the map F has a chaotic attractor on S.

trajectory enters the region R_3, and after one iteration under F_3 we again have a point on $L_0^{(1)}$. As it was shown in Sushko et al. (2004) (see also Sushko and Gardini, 2009) the dynamics of F in such a case can be either periodic, or quasiperiodic.

- The trajectory, starting from the point $(k_{j+1+s}, y_{j+1+s}) \in R_2$ after a number of consecutive points in R_2 (with $k < 0$) enters the region R_1 (indeed, the trajectory can enter only subregions not belonging to Z_0). Then, using our analysis in Appendix A, related to the images of R_i, we can state that the trajectory, after a number of consecutive points in R_1, must enter the subregion R_2 with $k > 0$ and then the region R_3. As in the previous case, after one iteration under F_3 the trajectory comes back to the straight line $L_0^{(1)}$.

An important conclusion from the above considerations (besides the existence of a backward mechanism for obtaining a generic trajectory of F) is that the map F_3 is always involved in the asymptotic dynamics of F, and that, due to its zero eigenvalue, there exists a one-dimensional subset S of the phase plane, to which the dynamics of F are reduced. Such a subset S is a broken line of two branches consisting of images of a proper segment of $L_0^{(1)}$. In the case $c < c^*$ the set S has a rather simple structure, which is in some sense similar to a piecewise linear approximation of the two branches of a hyperbola (see Fig. 5a), while for $c > c^*$ it can have a quite complicated structure with self-intersections and foldings (see an example in Fig. 5b). The main result of this analysis is the existence of a proper segment of $L_0^{(1)}$ to which we can restrict our study. The segment is given by $[a_0, a_1] \subset L_0^{(1)}$, where the point a_0 is the intersection between the two straight lines $L_{-1}^{(1)}$ (whose equation is given above: $y = 1 - rk/a$) and $L_0^{(1)}$ (whose equation is given in Appendix A: $y = c - rk/(1 - r)$), that is: $a_0 = (a(c - 1)(1 - r)/r(a - 1 + r), (a - c(1 - r))/(a - 1 + r))$. While a_1 is its image under the map, $a_1 = F(a_0)$, which belongs to the line $L_0^{(1)}$ and to its image under the map F. So, as described in the next section, just considering the one-dimensional return map on the segment $[a_0, a_1]$ we can investigate and explain the main properties of the map F.

3. Dynamics of the return map

We present here some properties and numerical results related to the dynamics of the first return map $\varphi : [a_0, a_1] \to [a_0, a_1]$. Let us first define it:

Definition 1. The first return map $\varphi : [a_0, a_1] \to [a_0, a_1]$ is a map φ through which the k-coordinate of a given point $(k, y) \in [a_0, a_1]$ is mapped to the point $\varphi(k)$ which is the k-coordinate of the first point satisfying $F^n(k, y) \in [a_0, a_1]$.

The map $\varphi(k)$ is a piecewise smooth function which has, in general, a number $n_1 \geq 1$ of kink points. These are the k-coordinates of the images of the intersection points of the invariant attracting set S with $L_{-1}^{(1)}$ and $L_{-1}^{(2)}$ that belong to $[a_0, a_1]$. Further $\varphi(k)$ has some number $n_2 \geq 1$ of discontinuity points. These are the k-coordinates of images of the intersection points of the invariant attracting set S with the line of non definition $y = 0$ that belong to $[a_0, a_1]$.

A fixed point of the map $\varphi(k)$ corresponds to a cycle of some period n of the map F. The m th return on $[a_0, a_1]$ is given by the map φ^m. If the map F has a cycle of period n with m points in the segment $[a_0, a_1]$, then the m th return map φ^m has m fixed points.

Fig. 6 shows two return maps $\varphi(k)$ related to the parameter values of Fig. 5a and b, respectively. The return map shown in Fig. 6a corresponds to the case in which the map F has an attracting and a saddle cycle of period 8, so that the related return map $\varphi(k)$ has one attracting and one repelling fixed point. The map $\varphi(k)$ has one kinked point and one point of discontinuity.

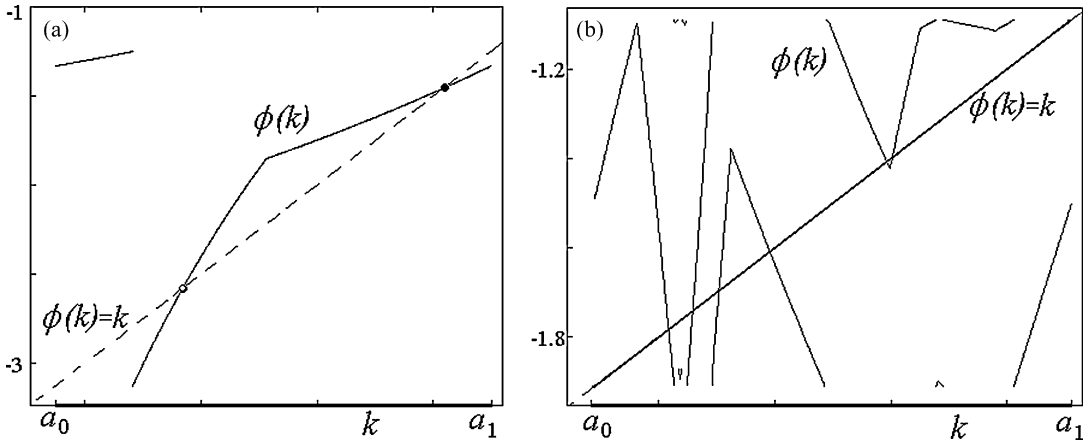

Fig. 6. Return map $\varphi(k)$ at $r = 0.3$, $c = 0.41$, $a = 1.25$ (a) and $a = 2.5$ (b).

The return map shown in Fig. 6b has a more complicated structure, with 9 kink points and 9 points of discontinuity. The fixed points of $\varphi(k)$ are all repelling, and no stable cycle can exist as the derivative is $|\varphi'(k)| > 1$ in all the points of the absorbing segment, which proves that the attracting set in Fig. 5b is chaotic.

Using the first return map $\varphi(k)$ we can study the bifurcations occurring to the attractors of the map F. Due to the structure of the return map, which is piecewise smooth, with kinked points and discontinuity points, cycles may appear, or bifurcate (i.e. a stable cycle may become unstable) due to the eigenvalue, or it may undergo a border-collision bifurcation, as the parameters are changed. This occurs when a periodic point of a cycle merges with a kinked point or a point of discontinuity, after which the cycle no longer exists, and some other asymptotic behavior emerges.

Hence, besides the standard bifurcations (fold and flip), we have bifurcations related to the appearance/disappearance of cycles, or directly of chaotic attractors due to border-collision bifurcations. We cannot easily predict what occurs at a border-collision bifurcation of a cycle. In general this depends on the slopes of the functions at the kinked point or the point of discontinuity. This kind of bifurcations in piecewise smooth and discontinuous maps is a new research area. We refer to Avrutin and Schanz (2006) and Avrutin et al. (2006), for some works related to a one-dimensional discontinuous normal form, and to Maistrenko et al. (1995) for the bifurcations related to a continuous piecewise linear map. Here we do not discuss this problem in deeper detail: In our applied context we have simply verified numerically that several bifurcations of this kind occur for the cycles of the piecewise smooth discontinuous first return map, and thus for the map F.

As shown in Sushko et al. (2004), in the case $c < c^*$ an attracting cycle of the map F can only undergo a border-collision bifurcation. Consider, for example, the parameter values $r = 0.3$, $c = 0.41$, $a = 1.25$, for which the map F has an attracting 8-cycle and a saddle 8-cycle (see Fig. 5a); the related return map $\varphi(k)$ is shown in Fig. 6a.

Increasing the values of c the graph of $\varphi(k)$ moves down so that the two fixed points approach each other, and for $c \approx 0.436$ they merge, colliding with the kink point (see Fig. 7a), then disappearing and giving rise to a quasiperiodic trajectory. Thus, a "saddle-node" border-collision bifurcation occurs.

If the value of c is decreased, the attracting fixed point moves towards the boundary point a_1, and the repelling fixed point approaches the boundary point a_0 (and, simultaneously, the point of discontinuity tends to a_0 as well), so that at $c \approx 0.394$ a border-collision bifurcation of a different kind occurs (see Fig. 7b) again giving rise to a quasiperiodic trajectory. *Indeed, the boundaries of the regions of periodicity in the* (a, c)*-parameter plane, shown in* Figs. 2 and 3 *for* $c < c^*$*, are related to the two kinds of border-collision bifurcations, described above.*

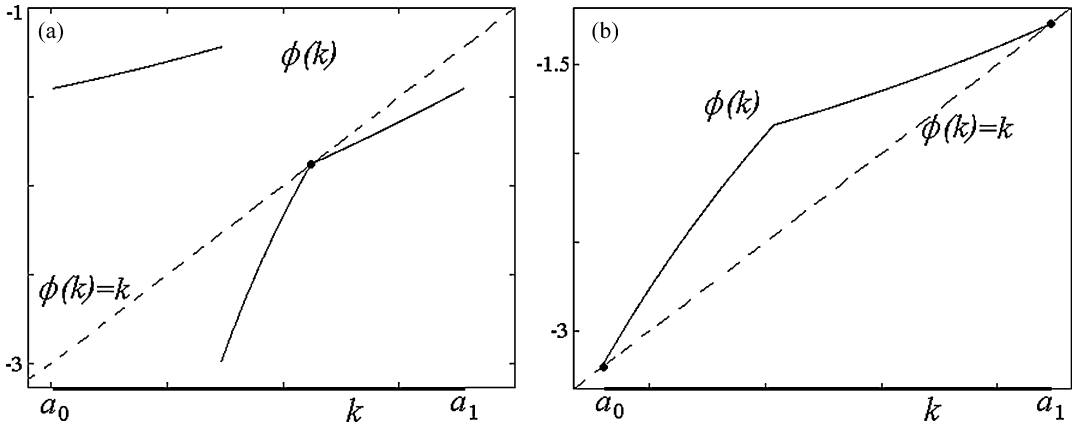

Fig. 7. Return map $\varphi(k)$ at $r = 0.3$, $a = 1.25$, $c = 0.436$ (a), and $c = 0.394$ (b).

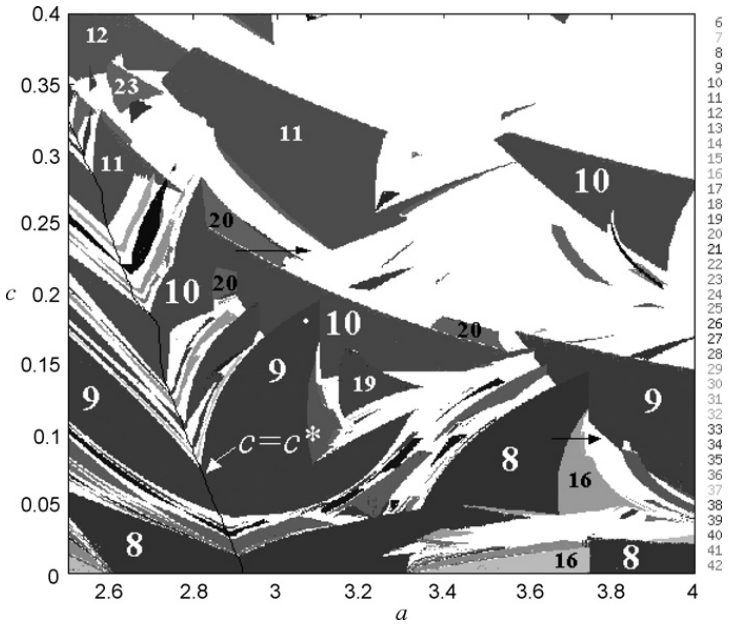

Fig. 8. The enlarged window of Fig. 2.

In order to show which kinds of bifurcations an attracting cycle of F can undergo for $c > c^*$, in Fig. 8 we show an enlargement of the rectangle in the lower right hand corner of Fig. 2, and consider several bifurcation sequences, related to the parameter changes indicated by the two straight lines with arrows.

So, let us first fix $r = 0.025$, $c = 0.23$, $a = 2.93$. For these parameter values the map F has a pair of 10-cycles, an attracting node and a saddle. The related return map $\varphi(k)$ has two fixed points, one attracting and one repelling (see Fig. 9a). Increasing a, at $a \approx 2.9369$ the attracting fixed point of $\varphi(k)$ undergoes a degenerate flip bifurcation (see Fig. 9b in which the map $\varphi^2(k)$ is shown close to this bifurcation). Exactly at the bifurcation value the map $\varphi(k)$ has an interval of period-2 points (i.e. all the points of the interval belong to 2-cycles, stable but not attracting), whereas after the bifurcation only one attracting 2-cycle is left (corresponding to two attracting fixed points of $\varphi^2(k)$ as shown in Fig. 10a). The related map F has an attracting 20-cycle. At $a = 3.0195$ the map $\varphi(k)$ has already two coexisting attractors: attracting 2- and 4-cycles. The attracting 4-cycle was born, together with a repelling 4-cycle, due to a "saddle-node" border-collision bifurcation: To see this, in Fig. 10b we show an enlargement of $\varphi^4(k)$. These two coexisting attractors of $\varphi(k)$ correspond to two different attracting cycles of the map F.

Besides the degenerate flip bifurcation of an attracting cycle, leading to a cycle of double period, we can have the "period-doubling" border-collision bifurcation. To show an example of such a bifurcation, let us fix the parameter values $r = 0.025$, $c = 0.1$, $a = 3.65$, for which the map F has an attracting cycle of period 8. The related return map $\varphi(k)$ is shown in Fig. 11a. Increasing a, at $a \approx 3.704$ the attracting fixed point of $\varphi(k)$ undergoes a "period-doubling" border-collision bifurcation giving rise to an attracting 2-cycle, which corresponds to an attracting 16-cycle of the map F (see Fig. 11b, which shows the map $\varphi(k)$ approximately at the bifurcation value).

If we continue to increase the value of a, one more "period-doubling" border-collision bifurcation occurs at $a \approx 3.7254$ (see Fig. 12a, in which the enlarged part of the map $\varphi^2(k)$ is shown approximately at the moment of this bifurcation). After

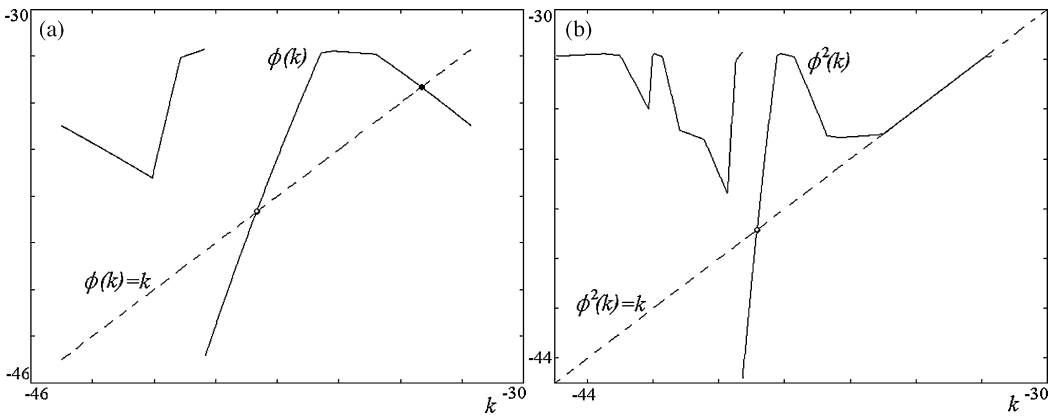

Fig. 9. Return maps, $r = 0.025$, $c = 0.23$, $a = 2.93$ (a); $a = 2.9369$ (b).

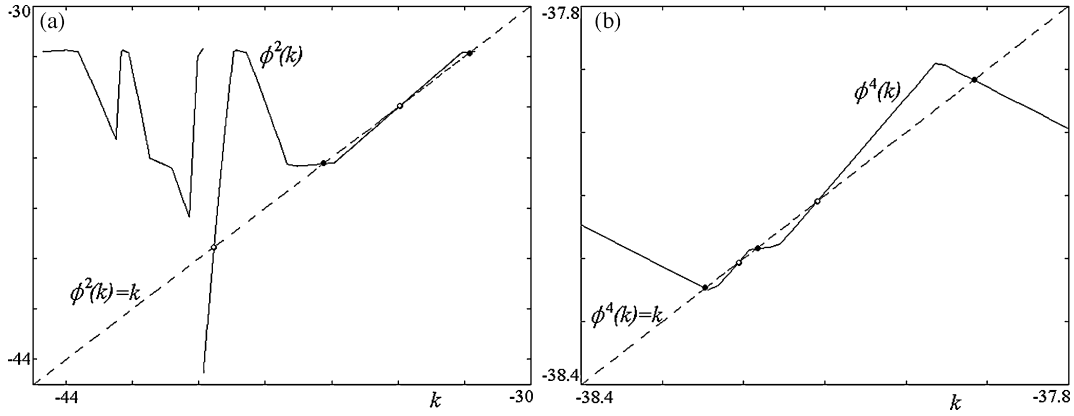

Fig. 10. Return maps, $r = 0.025$, $c = 0.23$, $a = 2.97$ (a); $a = 3.0195$ (b).

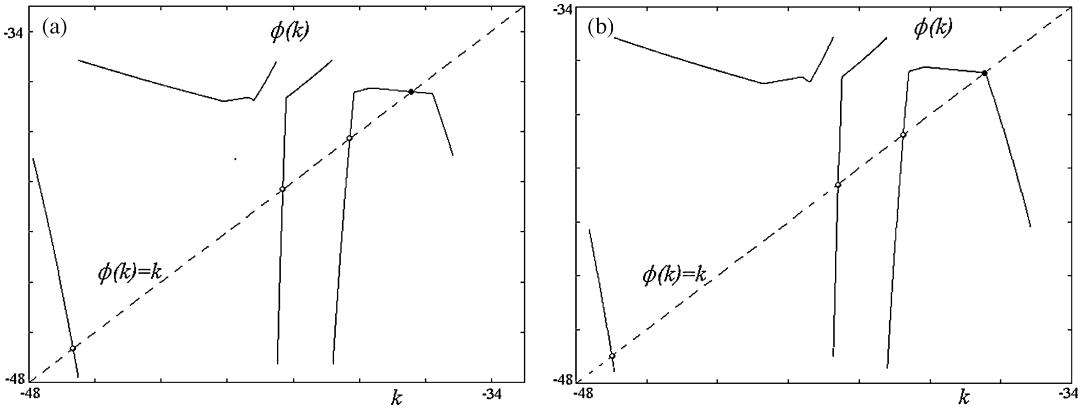

Fig. 11. Return maps, $r = 0.025$, $c = 0.1$, $a = 3.65$ (a); $a = 3.704$ (b).

the bifurcation the map $\varphi(k)$ has an attracting cycle of period 4, corresponding to an attracting 32-cycle of the map F. The next border-collision bifurcation occurs for the 4-cycle of $\varphi(k)$ at $a \approx 3.7371$, when a point of this cycle collides with a point of discontinuity, which leads to a chaotic attractor (see Fig. 12b), corresponding to a 9-piece cyclical chaotic attractor of the map F shown in Fig. 13a.

In Fig. 13b we show an enlargement of the phase plane indicated in Fig. 13a by a rectangle containing three pieces of the 9-piece cyclical chaotic attractor. It can be seen that one piece of the attractor intersects the line of discontinuity $y = 0$, so its image consists of two unbounded pieces of the attractor belonging to $L_0^{(1)}$.

From one single example we have thus shown that for $c > c^*$ an attracting cycle of the map F, besides the "saddle-node" border-collision bifurcation, can also undergo a degenerate flip bifurcation, and a "period-doubling" border-collision bifurcation, as well as a border-collision bifurcation leading directly to chaos.

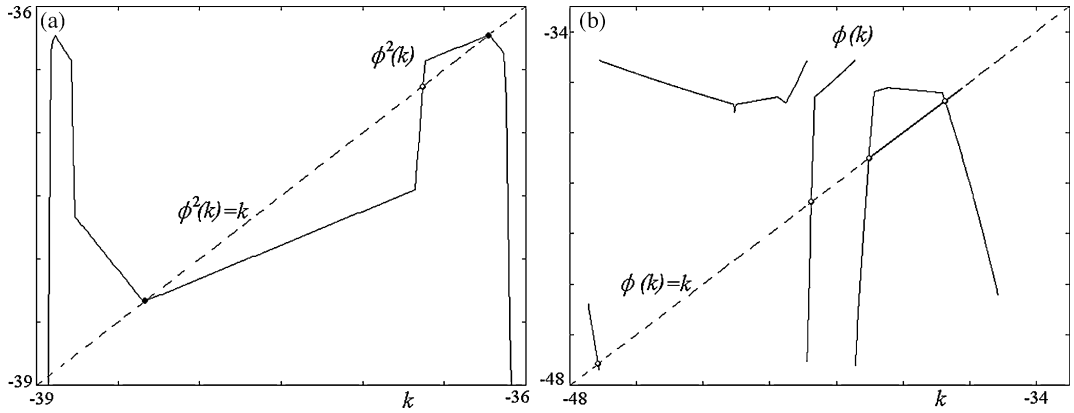

Fig. 12. Return maps, $r = 0.025$, $c = 0.1$, $a = 3.7254$ (a); $a = 3.738$ (b).

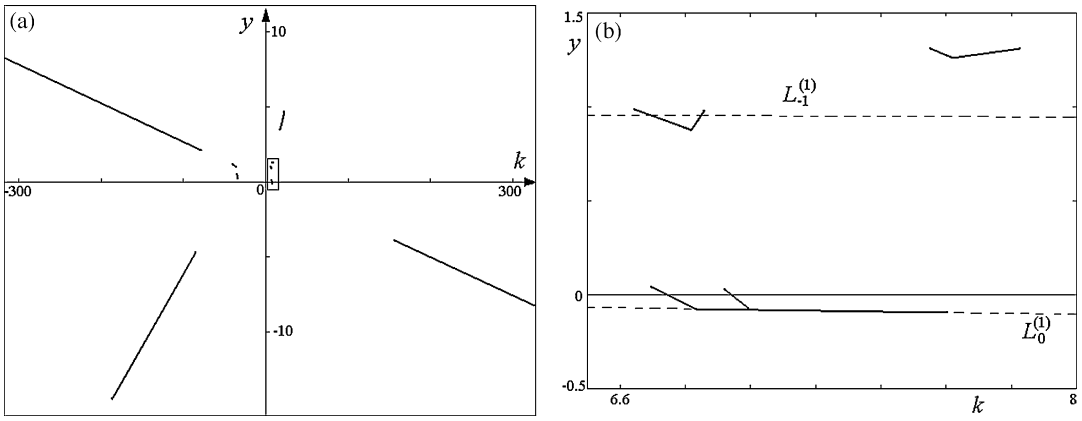

Fig. 13. The 9-piece cyclical attractor of the map F (a) at $r = 0.025$, $c = 0.1$, $a = 3.738$ in the phase plane; and (b) an enlargement of the rectangle.

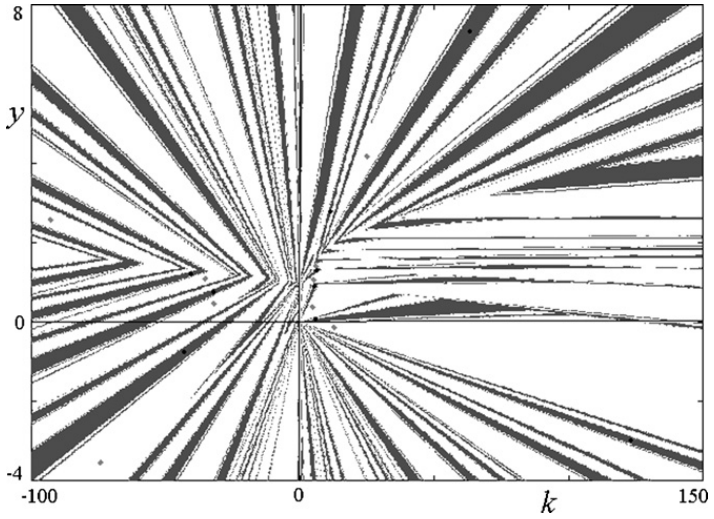

Fig. 14. Basins of attraction, $r = 0.025$, $c = 0.19$, and $a = 3.1$.

One more important difference of the case $c > c^*$ compared to $c < c^*$, is worth noting, namely that the regions of periodicity can overlap. This corresponds to bistability. The previous example also showed this property of bistability.

As another example, let us consider the parameter values in the point inside the 9- and 10-periodicity tongue (or region of periodicity) shown in Fig. 8. Then 9- and 10-cycles of the map F coexist in the phase plane, and in Fig. 14 we show the related two basins of attraction.

An enlarged part in Fig. 15 shows that the frontier between the two basins may have a fractal structure. Hence, the noninvertibility of the map F, together with the possible existence of chaos and chaotic repellors, leads to the complex structure of the basins of attraction, with pieces which may be disjoint. Moreover, it is of some interest to note that for high values of a we mainly observe chaotic dynamics, and that the structure of the chaotic invariant set becomes more and more folded as the number of intersections with $L_{-1}^{(2)}$ increases. As an example to illustrate the complex structure of an attractor of the map F, we show the enlargement of the attractor at $r = 0.3$, $c = 0.5$, $a = 15$ in Fig. 16.

4. Growth rates

The preceding sections concerned the dynamics for the evolution of the "relative" variables k_j, y_j, as only these could produce stationary orbits in a growing system. These were, however, only introduced for analytical purposes. What the economists are really interested in is the orbit for K_j, Y_j, in particular Y_j.

We can note that, whenever there is an attracting cycle of period n, with periodic points (k_j, y_j), $j = 1, \ldots, n$, then from (18) for any j, the product

$$\frac{Y_{j-1+n}}{Y_{j-1}} = y_j y_{j+1} \cdots y_{j+n} = y_1 y_2 \cdots y_n, \tag{28}$$

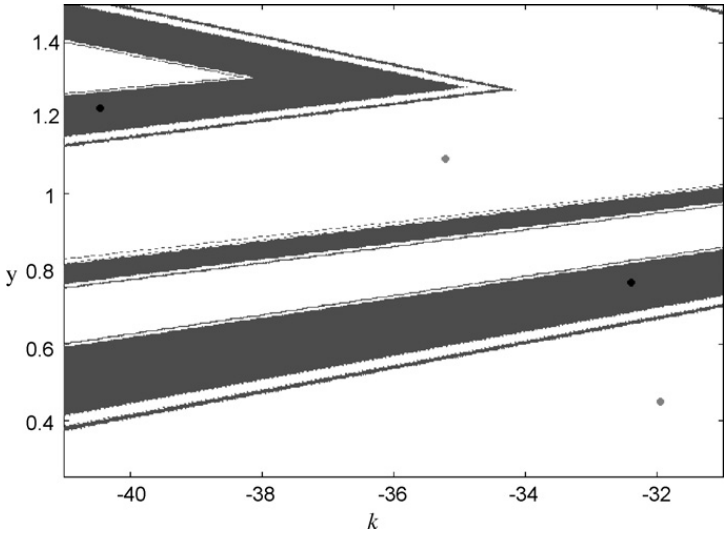

Fig. 15. The enlarged window of Fig. 14.

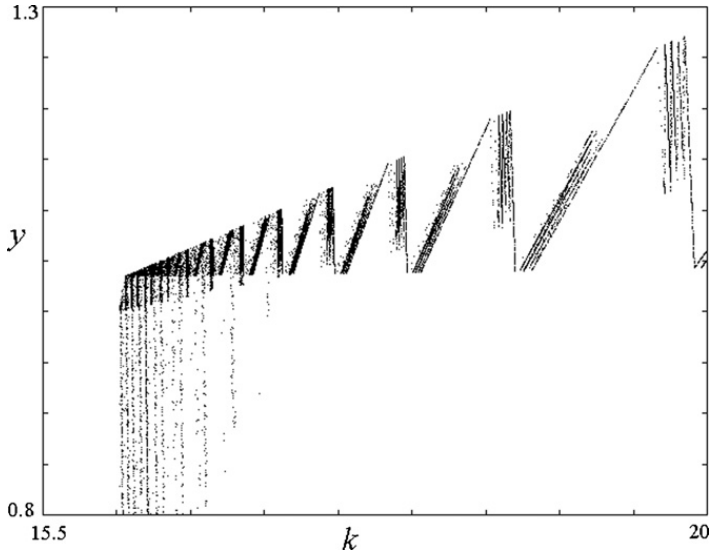

Fig. 16. Enlargement of a chaotic attractor in the phase plane, at $r = 0.3$, $c = 0.5$, and $a = 15$.

is an invariant which equals the growth factor of income (growth rate augmented by unity) over one complete cycle. We can now replace the expressions $y_j y_{j+1} \cdots y_{j+n}$ or $y_1 y_2 \cdots y_n$ in (28) by their absolute values.[7] To obtain the growth rates reduced to a one period basis write

$$(1+R)^n = \left| \frac{Y_{j-1+n}}{Y_{j-1}} \right| = |y_1 y_2 \cdots y_n|. \tag{29}$$

For computational reasons, for any period−n cycle with $n \leq 42$ we calculate R from (29) as follows:

$$\ln(1+R) = \frac{1}{n} \ln |y_1 y_2 \cdots y_n| \tag{30}$$

$$R = \exp\left[\frac{1}{n} \ln |y_1 y_2 \cdots y_n| \right] - 1 \tag{31}$$

Whenever $R > 0$ we deal with growth, otherwise the income trend is decreasing, and numerical evidence indicates that for $a > 1$ we indeed deal with growth.

To get a picture of the growth rates corresponding to the regions of periodicity in Figs. 2 and 3, we calculated R for these, and pictured the growth rates in different gray shades in Figs. 17 and 18, respectively. Without any formal justification,

[7] The reason the absolute value works is that, should we have $y_1 y_2 \cdots y_n < 0$, then we can take the evolution over two cycles, for which $(y_1 y_2 \cdots y_n)^2 = |y_1 y_2 \cdots y_n|^2$.

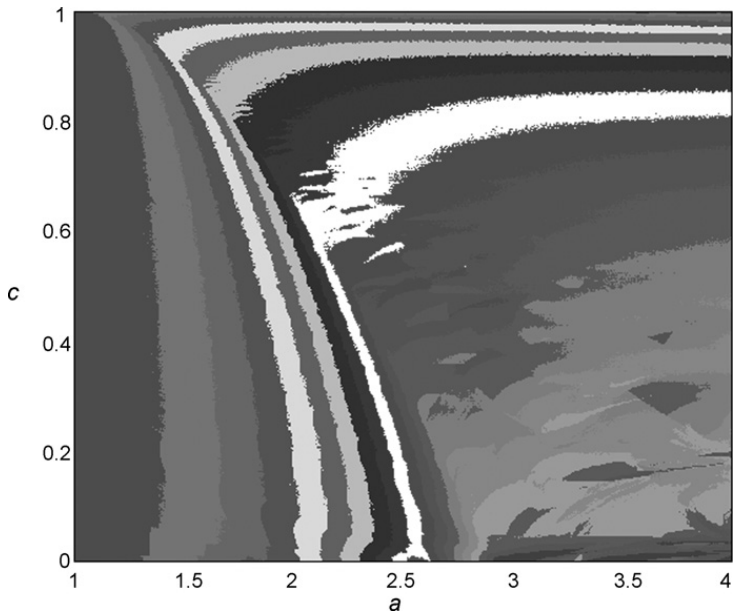

Fig. 17. Growth rates in the (a, c)-parameter plane at $r = 0.025$. The width of each band of different shades of gray corresponds to a growth rate of 0.007.

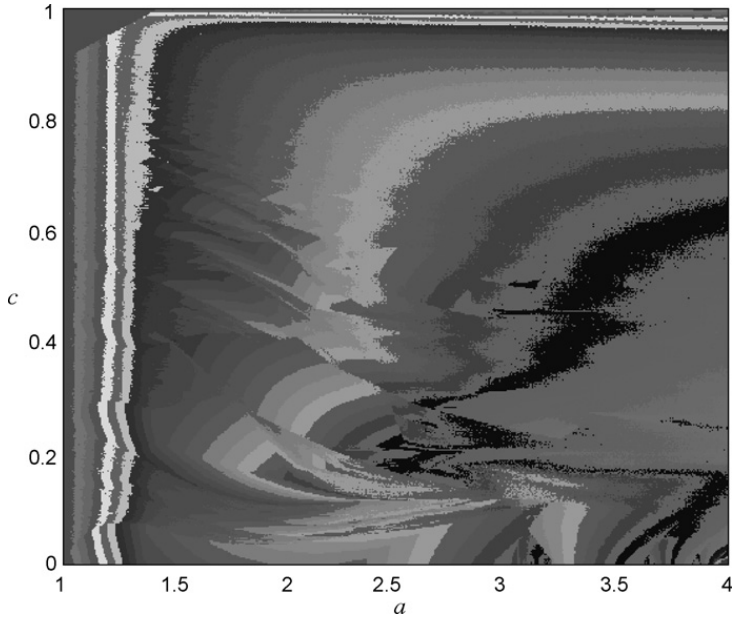

Fig. 18. Growth rates in the (a, c)-parameter plane at $r = 0.3$. The width of each band of different shades of gray corresponds to a growth rate of 0.007.

we also extended the idea to the cases of aperiodic or chaotic trajectories, and computed R with the same formula in (31) taking $n = 1500$, after a transient of 10,000 steps, and so extended the pictures of growth rates outside the domains of strict periodicity tongues. As we see, the rates of growth are radically reduced as compared to the growth rates for the original multiplier accelerator models.[8]

Examples of growth trends and income time series are shown in Fig. 19a and b resulting from the parameters $r = 0.025$, $c = 0.2$, and $a = 3.7$ (with $R = 0.1036245$) and $a = 4.0$ (with $R = 0.1099578$), respectively.

[8] To appreciate this point it must be recalled that the original multiplier/accelerator model $Y_j = (a + c)Y_{j-1} - aY_{j-2}$ does not have any growth trend in the oscillatory solution $Y_j = \rho^t \cos(\omega j + \varepsilon)$, where $\rho = \sqrt{a}$, does not have any growth term. The exponential factor ρ^t is an envelope for the cyclic variation around a *stationary* income level. Yet, we may note that this growth rate (50% *per period* for $a = 2.25$, 100% for $a = 4$) is huge. The original model can only produce pure growth (without oscillations) $Y_j = A_1\lambda_1^j + A_2\lambda_2^j$ at the rates $\lambda_{1,2} = (1/2)(a + c) \pm (1/2)\sqrt{(a + c)^2 - 4a}$, of which the largest dominates eventually. This is growth of an equally huge magnitude.

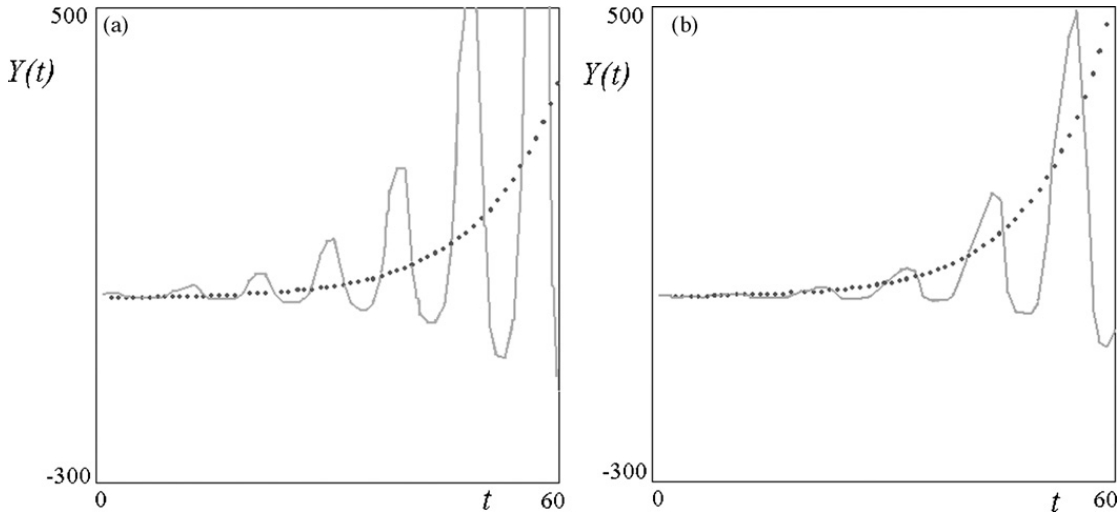

Fig. 19. The trajectory $Y(t)$ and the function e^{Rt} at $r = 0.025$, $c = 0.2$, $a = 3.7$, $R = 0.1036245$ (a); $a = 4$, and $R = 0.1099578$ (b).

5. Conclusion

In a previous paper, Puu et al. (2005), the authors considered a possibility of reassembling the Hicksian trade cycle model in a new way. The floor was tied to the stock of capital through a given rate of depreciation, thus rendering a lower bound to disinvestment when no worn out capital was replaced. For this reason the stock of capital had to be included as a new variable in the model. It was not in the original model, Hicks (1950), but, as capital is the cumulative sum of all past net investments, and, as the determinants of investment were an important part of the model, no additional elements were needed to achieve the inclusion of capital, and so close the model.

As a result, the model could create a growth trend along with growth rate cycles endogenously, which had been impossible in the original model, where an exogenous growth trend in autonomous expenditures had to be added. The setup called for a new method in order to deal with a growing system, through converting it to "relative" variables; the income growth factor and the capital/income ratio. A full mathematical analysis was supplied in Sushko et al. (2004) (see also Sushko and Gardini, 2009).

The model could produce periodic or quasiperiodic orbits, and also had the advantage that the enormous income growth rates of Samuelson's and Hicks's models were reduced by about a factor of one hundredth in the periodic and quasiperiodic regimes. However, for high values of the accelerator, pure exponential growth (at the original high rates) remained, quite as in Samuelson (1939) and Hicks (1950).

In a recent publication, Puu (2007), one of the present authors reintroduced the ceiling, again using capital stock as an actual capacity limit for producing real income. It was demonstrated that the pure growth cases no longer existed, and numerical experiments indicated both chaos and multistability, but the numerical results remained inconclusive, and the model itself largely mathematically unexplored.

The aim of the present contribution is to provide a full mathematical analysis of the new model in Puu (2007). A full description of the mathematical properties of the different branches of the map are given in Appendix A. Its was shown that chaos and multistability indeed occur in the new model, and a variety of bifurcation scenarios were explored. A numerical investigation indicated a drastic reduction of growth rates from the original huge values over the entire parameter space.

A full understanding of the working of the four-piece (originally three dimensional, two dimensional in relative variables) piecewise smooth map was attained by using a reduction to a one-dimensional return map.

Appendix A.

In this Appendix we first describe the dynamic behavior of each map F_i, $i = 1, 2, 3, 4$, given in Section 2, and then the dynamic behavior of the map in the phase plane.

- The map F_1 is an invertible map having two fixed points $(a, 1)$ and $(a, -1)$ with eigenvalues $\eta_{1,2} = \pm 1$ and $\eta_1 = \eta_2 = -1$, respectively. It maps the strip $\{(k, y) : -1 \le y \le 1\}$ in two half planes

$$\{(k, y) : y \ge k/a\} \quad \text{and} \quad \{(k, y) : y \le k/a - 2\},$$

while two half-planes $\{(k, y) : y \ge 1\}$ and $\{(k, y) : y \le -1\}$ are mapped by F_1 in the strips

$$\{(k, y) : k/a - 2 \le y \le k/a - 1\} \quad \text{and} \quad \{(k, y) : k/a - 1 \le y \le k/a\},$$

respectively. The straight line in between, denoted L_∞,

$$L_\infty = \{(k, y) : y = k/a - 1\},$$

is the image of the Poincaré Equator.

- The map F_2 is an invertible map of triangular type, such that y is mapped independently on k by a one-dimensional map f:

$$f : y \mapsto (c + a) - \frac{a}{y}. \tag{32}$$

It has two fixed points y_+ and y_-: $y_\pm = (c + a \pm \sqrt{(c+a)^2 - 4a})/2$, appearing at $c = c^{**} = 2\sqrt{a} - a$ via a saddle-node bifurcation. For $0 < c < c^{**}$ the map f has no fixed points, but any initial value y_0 is either n-periodic with rotation number m/n (for $c = 2\sqrt{a}\cos(\pi m/n) - a$) or quasiperiodic with rotation number ρ (for $c = 2\sqrt{a}\cos(\pi\rho) - a$) (see Sushko and Gardini, 2009). An eigenvalue of f is $\lambda_1(y) = a/y^2$. If the fixed points $y_\pm$ exist, i.e., for $c \geq c^{**}$, we have $0 < \lambda_1(y_+) < 1$ and $\lambda_1(y_-) > 1$. The corresponding fixed points of the map F_2 are (a, y_-) and (a, y_+). Indeed, it can be easily checked that the straight line $\{x = a\}$ is invariant under the map F_2. Moreover, in Sushko and Gardini (2009) it is shown that this line is transversely attracting for $a > 1$ and transversely repelling for $a < 1$; Any point (a, y) is either periodic, or quasiperiodic; At $a = 1$ any point (k_0, y_0) is either periodic, or quasiperiodic, and any trajectory belongs to corresponding invariant hyperbola. The second eigenvalue of F_2 is $\lambda_2(y) = 1/y$. Taking into account that $c \geq c^{**}$ the inequalities $\lambda_2(y_+) < 1$ and $\lambda_2(y_-) < 1$ hold (as $c > 2 - a$), we have that the fixed point (a, y_+) is an attracting node and (a, y_-) is a saddle (and both belong to the region R_1). Let $L_0^{(2)}$ denote the image of $L_{-1}^{(2)}$ by F_2, i.e.,

$$L_0^{(2)} = F_2(L_{-1}^{(2)}) = \left\{(k, y) : y = \frac{(k + c)}{(a + 1)}\right\}.$$

- Consider now the map F_3. Due to one zero eigenvalue in each part of the definition, any point of the phase plane is mapped by F_3 into a point of a straight line, denoted $L_0^{(1)}$,

$$L_0^{(1)} = F_3(L_{-1}^{(1)}) = \left\{(k, y) : y = \frac{c - rk}{(1 - r)}\right\},$$

on which the map F_3 is reduced to a one-dimensional map g:

$$g : k \mapsto g(k) = \frac{k(1 - r)^2}{c(1 - r) - rk}. \tag{33}$$

The map g has two fixed points: $k^* = (1 - r)(c - 1 + r)/r$ and $k^{**} = 0$. If $c < 1 - r$, then k^{**} is repelling and k^* is attracting, while if $c > 1 - r$, then k^* is repelling and k^{**} is attracting. At $c = 1 - r$ these fixed points merge: $k^* = k^{**} = 0$. The corresponding fixed points of the map F_3 are (k^{**}, c) and $(k^*, (1 - r))$. The map F_3 is a noninvertible map of $(Z_0 - Z_\infty - Z_0)$-type.

- The dynamics of the map F_4 are trivial. Due to one zero eigenvalue, any point of the phase plane is mapped into a point of the straight line denoted $L^{(3)}$:

$$L^{(3)} = \left\{(k, y) : y = \frac{k}{a(1 - r)}\right\},$$

which in one more iteration is mapped into the fixed point $p_1 = (a(1 - r)^2, (1 - r))$ of F_4 (the second eigenvalue of the fixed point is also 0). Note that if $(k, y) \in L_{-1}^{(3)}$ then $F_4(k, y) = (k_1, y_1) \in L^{(3)}$, where $k_1 = (1 - r)ack/(ra + k)$, $y_1 = ck/(ra + k)$.

It is not difficult to check that for the parameter range considered, no one of the fixed points, mentioned above, of the individual maps F_i, $i = 1, 2, 3, 4$, belongs to the definition region of the related map.

A.1. Action of the map F

In order to understand the dynamic action of the map F (whose components have been considered separately in the above discussion), we have to understand how is the image of the phase plane under F. This will lead us to locate the regions where it is possible to get the invariant attracting sets, and the regions in which the map is invertible or noninvertible. We recall that the phase space may be subdivided in regions, or zones, Z_k such that each point of a region Z_k has k distinct rank-one preimages (see Mira et al. (1996) for more details). A region Z_0 denotes points having no rank-one preimage (which also

means that a point can never be mapped in such a region, and thus no limit set can belong to it). A region Z_∞ denotes points having infinitely many rank-one preimages, as it occurs in maps having degenerate cases, as straight lines mapped into points, as it is in our case.

So, let us describe the images of the regions R_i, $i = 1, 2, 3, 4$, by F: if a region is not visited by $F(R_i)$, $i = 1, 2, 3, 4$, then it is a region Z_0; if a region includes points of $F(R_1)$ and of $F(R_2)$ then it is a region Z_2.

As the boundaries of the regions R_i are the lines $L_{-1}^{(i)}$, the regions $F(R_i)$ are bounded by the images $F(L_{-1}^{(i)})$. First note that lines $L_{-1}^{(1)}$, $L_{-1}^{(2)}$ and $L_{-1}^{(3)}$ (belonging to the boundaries of the regions R_i) intersect in the same point (see Fig. 1), which we denote p_0: $p_0 = (k_0, y_0) = L_{-1}^{(1)} \cap L_{-1}^{(2)} \cap L_{-1}^{(3)}$, $k_0 = ac/(1 + r(c + 1))$, $y_0 = 1 - rk_0/a$. The point p_1 is the image of p_0 under F, i.e., $p_1 = F(p_0)$. Obviously, $p_1 = L_0^{(1)} \cap L_0^{(2)} \cap L^{(3)}$. Now we can easily obtain an image of the region R_4, which is a segment: $F(R_4) = F_4(R_4) = (0, p_1]$. For our parameter ranges this segment $(0, p_1] \in R_3$ (see Fig. 4).

Now let us get the image of R_3. As mentioned above, F_3 maps any point of the plane into a point of the straight line $L_0^{(1)}$. So,

$$F_3(R_3) = \{(k, y) : (k, y) \in L_0^{(1)} \quad \text{for} \quad k < 0 \quad \text{and} k \geq k_1\}.$$

Note, that due to the intersection of $L_{-1}^{(1)}$ with the axis $y = 0$, we have a singularity point $s_0 = (a/r, 0)$. Let $(k_0, y_0) \in L_{-1}^{(1)}$, $F_3(k_0, y_0) = (k_1, y_1) \in L_0^{(1)}$. Then $y_1 \to \pm\infty$ as $y_0 \to 0\mp$, while points at infinity of $L_{-1}^{(1)}$ are mapped into a point, denoted s_∞, with coordinates $(a(1 - r)/r, c + a)$, that is, $y_1 \to (c + a)\mp$ as $y_0 \to \pm\infty$ (see Fig. 4).

The boundary $L_{-1}^{(2)}$ also intersects the axis $y = 0$ in a point denoted s_0': $s_0' = (-a^2, 0)$. If $(k_0, y_0) \in L_{-1}^{(2)}$ and $F_2(k_0, y_0) = (k_1, y_1) \in L_0^{(2)}$, then $y_1 \to \pm\infty$ as $y_0 \to 0\mp$; points at infinity of $L_{-1}^{(2)}$ are mapped into a point $s_\infty' = (a(c + a + 1), c + a)$, i.e., $y_1 \to (c + a)\mp$ as $y_0 \to \pm\infty$.

The images of the regions R_1 and R_2 are shown in Fig. 4 as gray and hatched regions, respectively. More precisely, the subregion of R_1 such that $k < 0, y > 0$, is mapped into the region above $L_0^{(2)}$ and below $y = 0$, i.e., into the region

$$\left\{(k, y) : \frac{(k + c)}{(a + 1)} < y < 0\right\}.$$

The subregion of R_1, such that $k < 0, y < 0$, is mapped into a region below $L_0^{(2)}$, below L_∞ and above $y = 0$, that is, into the region

$$\left\{(k, y) : 0 < y < \frac{k}{a - 1}, \quad \text{and} \quad y < \frac{(k + c)}{(a + 1)}\right\}.$$

Finally, the subregion of R_1 such that $k > 0, y > 0$ is mapped in the region

$$\left\{(k, y) : \frac{k}{a - 1} < y < \frac{(k + c)}{(a + 1)}, \quad \text{and} \quad 0 < y < \frac{k}{a(1 - r)}\right\}.$$

Let us now consider the image of the region R_2 in detail. Its part related to $k < 0, y > 0$ is mapped into the region given by:

$$\left\{(k, y) : \frac{(k + c)}{(a + 1)} < y < \frac{c - rk}{(1 - r)}, \quad \text{and} \quad (k + a) < y < (c + a)\right\}.$$

The subregion of R_2 such that $k < 0, y < 0$ is mapped into the following region:

$$\left\{(k, y) : (c + a) < y < \frac{(k + c)}{(a + 1)}\right\}.$$

The subregion of R_2 with $k > 0, y > 0$ is mapped in the region:

$$\left\{(k, y) : \frac{c - rk}{(1 - r)} < y < \frac{(k + c)}{(a + 1)}, \quad \text{and} \quad y < (c + a)\right\}.$$

Finally the image of the subregion of R_2 with $k > 0, y < 0$ is the region

$$\left\{(k, y) : (c + a) < y < \frac{c - rk}{(1 - r)}\right\}.$$

In order to illustrate the images of the regions R_i, $i = 1, 2, 3, 4$, in Fig. 4 we have taken $a = 2$, $c = 0.6$, $r = 0.3$, but it can be easily checked that for other parameter values in the range of interest the picture is qualitatively the same. From the same picture one can also get information about the invertibility of the map F, namely, points of the gray region have one preimage, as also do points of the hatched region (denote these regions as Z_1); in the overlapping gray and hatched regions the related points have two preimages (Z_2); points of the white region have no preimages (Z_0). And clearly, as it was already mentioned above, due to a zero eigenvalue, the points of $L_0^{(1)}$ have infinitely many preimages (Z_∞). From this description we

also can see that the line of discontinuity $k = 0$, as well as the region R_4, have no influence on the asymptotic dynamics of the map F.

References

Avrutin, V., Schanz, M., 2006. Multi-parametric bifurcations in a scalar piecewise-linear map. Nonlinearity 19, 531–552.
Avrutin, V., Schanz, M., Banerjee, S., 2006. Multi-parametric bifurcations in a piecewise-linear discontinuous map. Nonlinearity 19, 1875–1906.
Hicks, J.R., 1950. A Contribution to the Theory of the Trade Cycle. Oxford University Press, Oxford.
Maistrenko, Y.L., Maistrenko, V.L., Vikul, S.I., Chua, L., 1995. Bifurcations of attracting cycles from time-delayed Chua's circuit. International Journal of Bifurcation and Chaos 5 (3), 653–671.
Mira, C., Gardini, L., Barugola, A., Cathala, J.C., 1996. Chaotic Dynamics in Two-Dimensional Noninvertible Maps. World Scientific, Singapore.
Puu, T., Gardini, L., Sushko, I., 2005. A Hicksian multiplier-accelerator model with floor determined by capital stock. Journal of Economic Behavior and Organization 56, 331–348.
Puu, T., 2007. The Hicksian trade cycle with floor and ceiling dependent on capital stock. Journal of Economic Dynamics & Control 31, 575–592.
Samuelson, P.A., 1939. Interactions between the multiplier analysis and the principle of acceleration. Review of Economic Statistics 21, 75–78.
Sushko, I., Gardini, L., Center bifurcation of a point on the Poincar é Equator. Proc. of ECIT 2008, Grazer Math. Ber. No. 354, 2009.
Sushko, I., Gardini, L., Puu, T., 2004. Tongues of periodicity in a family of two-dimensional discontinuous maps of real Möbius type. Chaos, Solitons & Fractals 21, 403–412.